AD NUMBER

AD845735

NEW LIMITATION CHANGE

TO

Approved for public release, distribution unlimited

FROM

Distribution authorized to U.S. Gov't. agencies and their contractors; Critical Technology; OCT 1968. Other requests shall be referred to Commanding Officer, Department of the Army, Fort Detrick, Attn: SMUFD-AE-T, Frederick, MD 21701.

AUTHORITY

Department of the Army, SMUFD/Fort Detrick ltr dtd 17 Feb 1972

TRANSLATION NO. 2340

DATE: 14 Oct 1968

DDC AVAILABILITY NOTICE

This document is subject to special export controls and each transmittal to foreign governments or foreign nationals may be made only with prior approval of Commanding Officer, Fort Detrick, ATTN: SMUFD-AE-T, Frederick, Md. 21701.

DEPARTMENT OF THE ARMY
Fort Detrick
Frederick, Maryland

THE FLOW LOSSES AT 90° TURNS IN PNEUMATIC DUST TRANSPORT

Brennstoff - Waerme - Kraft (Fuel, Heat, Power), Vol 19, No 9, 1967, pp 430-435.

R. Jung, Dr. of Engineering, Association of German Engineers ([VDI] Verein Deutscher Ingenieure), Head of the Research Institute for Flow and Process Technology at L & C Steinmueller Company (Stroemungs- und Verfahrenstechnische Versuchsanstalt der L & C Steinmueller GmbH), Gummersbach.

UDC: 621.867.82-492:533.6.011:532.552

Measurements of the pressure course in dust-laden air flows prior to and following curves of various configurations indicate the pressure drop caused in a permanent manner by the curve. This pressure drop is caused by the energy consumption during the reacceleration that follows the turn and is required to compensate for the friction that develops. The measured values characterize the transition between the ultimately developed states of the transport process before the turn and upstream.

Definition of the problem

A significant portion of the total pressure drop in the pneumatic transport of powdery substances is attributable to turns in the conveying flow. In the application cases to be discussed first, we shall mainly deal with continuously curved tube arcs and -- in the case of larger diameters -- with segmental curves or tube elbows with vanes that are easy to manufacture. The conveyor conduits investigated have nominal diameters of less than approximately 300 mm. No results of systematic studies of turn losses caused by the conveyed substance have been published so far.

G. Weidner [1] calculated the velocity loss of a grainy substance in a tube arc assuming that the entire substance flow glides along the back of the curve, subject to a friction loss caused by a composite effect of centrifugal force and the normal component of the weight of the substance, but not to propellance by the air flow. The corresponding flow loss is the same as the pressure drop that is consumed by the acceleration of the substance in the subsequent straight tube to the initial velocity as it enters the curvature. The results of this theory are -- within a relatively large scattering of the results -- about the same as the turn losses observed in the pneumatic conveyance of seedy fruits.

The author [2] established in an earlier report these losses in a 90° tube arc with various degrees of curvature for spherical cast-iron granules as the conveyed substance. The results of the measurements agreed roughly with the estimated values that correspond to a substance flow braked to zero velocity at the exit from the curve.

The main purpose of the tests described below is to elucidate some problems that pertain to the design of conveyance paths with relatively large diameter, such as coal dust pneumatic lines in large-scale firing installations. Accordingly, the investigation was restricted to low substance loadings. In the above-25 m/sec air velocity range selected for study, the gravitational force had a relatively insignificant effect on the conveyance process compared to the inertia resistance of the particles and to the conveying power of the air flow.

Experimental setup and method

The experimental setup is illustrated in Fig. 1. The conveying air laden with dust flows from the outside through the rounded entry a into the conveying system: the dust is added in a uniform manner at b. It flows through the measuring sites c and d, the precipitation cyclone e and effluent air exit f to the exhaust connection. The conveyed substance precipitated in e flows by itself from collecting vessel g into a closed flow through tube conduit h and thence into the open funnel i of a rotating tube dispenser k that may be adjusted for r.p.m. in a continuous manner and that effects the dosage of the substance admixed once again to the air flow. The substance column in tube h at the bottom open end of which the substance flows out freely into funnel i serves as a seal from the larger external pressure. The creeping flow that enters the system through this porous column is insignificantly low compared to the flow of the conveying air. The exhaust air flow is righted in tube f and is then measured further downstream with a standard diaphragm.

The turn loss in the 90° curvature 1 is obtained from the course of the static pressure in the straight measuring sections c and d, taken over a total of 45 small measuring tubes in the tube wall and indicated by a series manometer.

The turn losses established in preliminary tests on simple tube curves at air flow rates of somewhat more than 25 m/sec turned out to be independent of the fact whether the conveying flow turned in the horizontal plane, in the vertical plane or from one plane into the other. It was therefore possible to restrict all subsequent determinations to one given spatial configuration of curves, specifically, to vertical upflow turned into horizontal.

Fig. 2 illustrates the details of the test section, showing inlet tube a, exhaust tube b, and test curve c between these two tubes. The conveying tube has a diameter of D = 150 mm i.d. in the vertical section, converging to a lower diameter of 125 mm along a distance of 1 meter. In this manner it became possible to shorten considerably the length of the straight section required to perform the conveying function. The length of the horizontal runout section after the curve is about 7.5 m or 50 D. From among the pressure-measuring sites d, the first (A) is at the beginning of the test section and the second (B) at its end: these assume particular significance with respect to the pressure course, as shall be shown later.

Quartz and coal dust, pneumatically separated into a fraction with small particle size between approximately 0.05 and 0.3 mm, served as the test dust conveyed. Within these limits, the measured turn losses were found to be independent of particle type for all practical purposes. The particle-size analysis for the quartz dust -- that was used solely after the preliminary tests and exhibited very little internal friction -- indicated

a residue of	1.4	76	86	90% at a
mesh width of	0.16	0.1	0.063	0.04 mm.

The particles had a near spherical shape and smoothened the tube wall to such an extent after a short test period that the friction coefficients measured with unladen air conoformed to the laws governing hydraulically smooth tubes.

Characterization of the turn loss

Course of pressure in the tube.

Fig. 3 illustrates the pressure course in an example along a conveying path with $(p_A - p)$ as the difference between pressure p_A at the beginning of

the vertical measuring distance (A in Fig. 2) and pressure p at the distance of x from the intersection point of the tube axes at the curve. The two curves apply for equal air flowthrough.

In the entering flow before the curve and relatively distant downstream from the turn there develops a linear pressure drop with a constant decrease $\Delta p/\Delta x$. The extensions of the lines through the measuring points in these regions of developed flow determine, in their intersection points with ordinate $x = 0$, the pressure loss caused by the turn, $\Delta p_{U,0}$ or Δp_U. These pressure jumps effectuate the transition from the developed flow state before and after the turn. In this expression, the pressure differences Δp_{10} and Δp_{02} corresponding, for example, to the mixed flow in the linear pressure course, representing the distances x_{10} and x_{02}, respectively (as shown below in the figure), are independent of the turn configuration, so that the pressure jump Δp_U essentially characterizes the direction change of the flow.

On the basis of these considerations it is also possible to directly compare turn losses sustained in turns of various arc lengths, whereby the same pressure drop between identically located points (for example, 1 and 2 in Fig. 3) encompass the same turn loss Δp_U. In the other usually employed definitions of this loss [3, especially, p 788] in terms of the difference between the pressure drops between points 1 and 2, as well as the pressure drop in a straight tub of the same length, encompassing also the section along the center line f the tube arc as a partial distance, this assumption -- which is of importance in the present case -- does not apply.

The example discussed applies to a tube arc where the dust flows together into hard-to-separate strands as a consequence of the conduction at the curvature backs. Accordingly, the constant pressure drop establishes itself only after a relatively long distance downstream from the turn.

In the case of a somewhat shorter distance, the conveyed goods, braked in the turn, undergo acceleration once more after an elbow in the channel, as shown in Fig. 4. The dust channeled layerwise by the vanes offers a greater surface of attack to the air flow than do the individual strands behind the tube arc. As a consequence, a steeper pressure drop and -- further downstream -- a shorter transition in the linear range of pressure distribution will establish itself under the same conditions that are illustrated in Fig. 3 after the turn.

The tube friction coefficient in the literature

The constant pressure drop $\Delta p/\Delta x$ in the developed mixed flow by a straight tube at an angle of α to the vertical is expressed in the literature

in the following form [4; 5]:

$$\Delta p/\Delta x = q\,\lambda^*/D \qquad (1)$$

In this expression, q denotes the compression pressure of the air flow and λ^* denotes a coefficient that is analogous to the tube friction coefficient that encompasses, according to the expression

$$\lambda^* = \lambda_L + \mu(\lambda_{S,R} + \lambda_{S,G} \sin\alpha), \qquad (2)$$

the tube friction effect of the air (λ_L) and of the dust ($\mu\lambda_{S,G} \sin\alpha$).

The tube friction coefficient λ_L was obtained in the tests without dust ($\mu = 0$) from the pressure drop

$$(\Delta p/\Delta x)_{\mu=0} = q\,\lambda_L/D,$$

corresponding to the inclination of the extrapolation lines with respect to the upper curve in Figs. 3 and 4. The λ_L values obtained are plotted vs the Reynolds number

$$Re = w\,D/\nu \qquad (3)$$

of the air flow in Fig. 5, and compared with the Prandtl law

$$1/\sqrt{\lambda_L} = 2\log^{10}(Re\sqrt{\lambda_L}) - 0.8. \qquad (4)$$

The mean deviation of the measurement results from this law is within the limits that correspond to a measuring uncertainty of approximately $\pm$ 1.5%.

The friction coefficient $\lambda_{S,R}$ of the dust in the case of pneumatic fly conveyance is a function of the two Froude numbers

$$Fr = w/\sqrt{gD} \qquad \text{and} \qquad Fr^* = w_F/\sqrt{gD} \qquad (5)$$

where w denotes the air velocity and w_F denotes the equilibrium falling velocity of a representative dust particle [4; 5; 6]. As the value of the parameter Fr increases, the effect of the gravitational acceleration g becomes less of an influence on the movement of the substance in the tube. Thus, the friction coefficient $\lambda_{S,R}$ will assume a constant value above a boundary value of Fr that decreases with decreasing values of Fr*.

Comparison with the test results

In the tests, Fr was > 20, Fr* was < 0.5, and the related dust content was $\mu < 1.5$. Under these conditions, the pressure drop measurements ($\Delta p/\Delta x$) in the flow that developed in the horizontal tube ($\alpha = 0$) behind the channel elbow (Fig. 4) had the average value of

$$\lambda_{S,R} = 0.002 \tag{6}$$

which rougly was comparable to the values reported in the literature [4; 6].

The largest deviations from this value, representing but a correction in this case for the determination of the turn loss in comparison to the friction coefficient λ_L, were in the amount of $\pm$ 0.001 at the boundary of measuring uncertainty for the pressure drop Δp in the developed flow. For a satisfactorily accurate measurement of the pressure drop

$$(\Delta p/\Delta x)_2 = (p_2 - p_E)/(x_E - x_{02}),$$

the amount of remaining tube section downstream -- the length $x_E - x_{02}$ of which decreased with increasing dust content μ -- was too short in most of the curvatures investigated. For this reason, the inclination of the extrapolation lines E - 2' (Fig. 4) was calculated with λ_L from Fig. 5 by using the expression

$$(\Delta p/\Delta x)_2 = [q(\lambda_L + 0.002\,\mu)]/D. \tag{7}$$

From this and of the value of pressure p_E at the last measuring site ($x = x_E$) the extrapolated pressure at the ordinate $x = 0$ was

$$p_2' = p_E + (\Delta p/\Delta x)_2\, x_E. \tag{8}$$

In the vertical upflow before the curve, the pressure drop

$$(\Delta p/\Delta x)_1 = (q[\lambda_L + \mu\,(\lambda_{S,R} + \lambda_{S,G})])/D \tag{9}$$

establishes itself according to Equations (1) and (2) with $\alpha = 90°$. Under the assumption -- valid in approximation -- that the velocity of the dust and of the air are the same in the developed flow, the following expression applies for the coefficient $\lambda_{S,G}$ (that considers the weight of the dust) according to [6; 7]:

$$\lambda_{S,G} = 2/(Fr)^2, \tag{10}$$

where Fr denotes the Froude number according to Equation (5). If Fr > 20,

which was the case in all tests, the effect of weight disappears insofar as it affects wall friction. As a result, the friction coefficient $\lambda_{S,R}$ becomes independent of inclination angle α, and the numerical value established in the horizontal tube remains valid, according to Equation (6), for the vertical tube also. The friction coefficient $\lambda_{S,R}$ quoted by the author in an earlier report [7] and which corresponded with the values reported in [5], are obviously too high at $\lambda_{S,R} = 0.005$. It is likely that the flow was then not fully developed in the vertical measuring section.

The pressure drops $(\Delta p/\Delta x)_1$ obtained from Equation (9) with λ_1 from Fig. 5, $\lambda_{S,R} = 0.002$, and $\lambda_{S,G}$ as in Equation (10) agreed satisfactorily with the values measured in the vertical tube. Otherwise, the extrapolated pressure p_1' could be determined precisely in a direct manner from the linear pressure distribution measured up to the entry into the turn (Figs. 3 and 4).

Explanation of the symbols

D	tube diameter
R	Mean half diameter of the circular arc turn
$\dot{m}_L$	mass flow of the conveying air
$\dot{m}_S$	mass flow of the conveyed substance
p	static pressure
q	$=(\rho/2)w^2$ compression pressure of the conveying air flow
w	$= \dot{m}_L/(\rho \pi D^2/4)$ mean air velocity
x	length coordinate of the measuring section
Δp_U	pressure drop caused by the turn
ζ_U	$= \Delta p_U/q$ related turn loss
ζ_0, ζ_1	related turn loss for $\mu = 0$ and $\mu = 1$, respectively
ζ_S	$= \zeta_1 - \zeta_0$ contribution of the dust to the turn loss
λ	tube friction coefficient
μ	$= \dot{m}_S/\dot{m}_L$ related dust content (loading)
ν,ρ	mean values of kinetic viscosity and density of the conveying air in the measuring section.

The pressure drop $\Delta p_U = p_1' - p_2'$ was determined according to this method in a total of 24 model turns at air velocities between 25 m/sec and 45 m/sec and loadings between $\mu = 0$ and approximately 1.4. The related turn losses

$$\zeta_U = \Delta p_U/q \qquad (11)$$

turned out to be independent of the air velocity w and thus -- within the above-mentioned ranges corresponding to w within the above boundary values -- also of the Froude and Reynolds numbers that occurred in a relatively narrow scattering range of the test results. Accordingly, the only factor that

remains to be considered within this representation for the turn loss coefficient ζ_U is the relation between the related dust content μ and the turn loss.

Relations between pressure drop and dust content

The loss coefficients ζ_U determined at the above-mentioned two turns (Figs. 3 and 4) are plotted vs μ in Fig. 6. The results may be characterized by a line that satisfies the expression

$$\zeta_U = \zeta_0 + \mu\,(\zeta_1 - \zeta_0) \tag{13}$$

with the parameters

$$\zeta_U = \zeta_0 \text{ for } \mu = 0 \text{ and } \zeta_U = \zeta_1 \text{ for } \mu = 1.$$

The mean scattering of these lines, the inclination

$$\zeta_S = \zeta_1 - \zeta_0 \tag{14}$$

of which characterizes the turn loss caused by the dust, is $\pm$ 2.6% in the DIN tube arc later to be designated as No 1 (Table 1). The corresponding value is approximately $\pm$3.5% in the case of the channel elbow with guding vanes (No 22), and approximately $\pm$ 3.0% in the average of all measurements. This uncertainty that encompasses all measured fluctuations within the limits of

$$2.5\cdot 10^5 \geq \text{Re} \geq 4.5\cdot 10^5$$

and

$$20 \geq \text{Fr} \geq$$

overshadows the coefficients relating to the loss coefficient ζ_U within these ranges.

Only the tube arc with the mean half diameter R = 5D (No 3 in Table 1) deviated from the linear relation between the parameter ζ_U determined in accordance with the above method and loading μ, for values of $\mu >$ approximately 0.6. The dust strands developed in the gently curved turn were not fully resolved by the end of the horizontal measuring section, and thus the flow did not develop at the last pressure sampling site E (Fig. 2). As a result, the pressure p_E was the initial value for the pressure p_2' according to Equation (8): this was too high, so that too low ζ_U values were obtained.

The model turns and their loss coefficients

The turn configurations investigated

The configurations and dimensions of the turns investigated are s in Table 1. In models where square or rectangular connection cross secti changed to round ones, the transition element, made from sheet metal, hac shape as shown in Fig. 7. These connection elements are to be regarded as ponent parts of the turns, since the individual parameters ζ_0 and ζ_1 incor rate the losses in the transition turn.

In the segment turns, n denotes the number of segments, with the connecting elements being counted as one segment. As shown in Fig. 8, the elbow planes intersect in a pole with the angles of $\Delta\varphi = 90°/n$. The first and the last of these planes form the angle of $\Delta\varphi/2$ with the perpendicul planes of the adjoining tube.

The four-edge tube arcs with square or rectangular cross section ture a much lower degree of local attrition in comparison with circular t turns, and also the ability of being made of thick-walled material where the risk of attrition is high (such as at the turn backs).

The channel elbow with square connection cross section, rounded c ners, and curved guiding vanes (Nos 21 and 22) corresponds to turns in la air and gas conduits such as are found in steam generators where for the of simplicity circular-cylindrically bent 90° vanes were selected. One co guration shaped in consideration for simplified construction with such a is the channel elbow with chamfered corners and plane guding sheets (Nos and 24).

The turn loss in pure air flow

The related turn loss

$$\zeta_0 = \Delta p_{U,0}/q$$

in a non-loaded air flow ($\mu = 0$) depends solely on the Reynolds number the tube flow for a given turn configuration. The test results for a cir lar tube arc were described comprehensively by H. Richter [8]. The corre ponding parameters ζ_0' relate to a representation of the pressure course which the ordinate $x = 0$ is determined by the center of the evolved arc than by the intersection of the two tube axes (Figs 2 to 4). In the 90° the value ζ_0' differs from the loss coefficient ζ_0 in Table 1 by the rela wall friction pressure drop

$$\zeta_0' - \zeta_0 = \lambda_L \, (2 - \pi/2) \, R/D$$

in a tube section that equals the difference between the shanks of the right angle and the inscribed quarter-circle arc with half diameter R. For the turns investigated here, this correction is within the scattering range of the results reported in [8]. Their remarkable divergence is a manifestation of even slight experimental errors on the pressure drop $\Delta p_{U,0}$ obtained by extrapolation. Accordingly, the relation between the parameter ζ_0 and the Reynolds number was overshadowed by measuring inaccuracies in the present tests also.

Larger turn losses are caused by the fact that the flow detaches itself from the inner sides of the turn wall. Accordingly, the loss coefficient ζ_0 of the tube elbow (No 4) is quite high. Much smaller turn losses are evident in the segmental turns as a result of lesser detachment (Nos 5 to 8); these values differ little from the losses in continuously curved tube arcs if the number of segments is $n > 3$ (Nos 9 and 10).

The smallest loss coefficient ζ_0 was measured in the four-edge tube arc No 12. In this arc, the flow decelerates according to the cross section increase of $(\pi/4)\, D^2$ in the tube to D^2 within the turn, so that the turn loss becomes smaller in comparison to the circle tube arc with same curvature (No 2). If the half diameter of the curvature is small, R, (No 11), this effect of velocity decrease is not evident as a consequence of the detachment of the flow at the inner side of the turn. An additional conveyance of the flow in an otherwise equal turn by means of an intermediate wall (No 13) has a similarly beneficial effect as an increase in the half diameter R. This deliberate improvement is not realized, however, if R is large to start with. Thus, the additional friction losses overwhelm the detachment losses that decrease at the intermediate wall (No 14).

In the four-edge tube arc with square cross section (No 15 and 16) the very same loss coefficients ζ_0 are obtained as in the circular tube arcs. The same applies also to a model with a cross section that increases towards the turn diagonal (Nos 17 and 18).

In the four-edge tube elbow (No 19), detachment of the flow at the inner edge causes a large turn loss, same as it does in the circular tube elbow (No 4). This loss decreases markedly if the circumflowed edge is rounded (No 20). Curved guding vanes cause a further decrease of this loss (Nos 21 and 22). On the other hand, inclined chamfering of the guding sheets and the incorporation of guding sheets at an angle (Nos 23 and 24) are less favorable in this respect.

The turn loss caused by the dust

The turn loss caused by the dust is shown in the last column of Table 1 as the parameter ζ_S. In this respect, the circular tube arc No 2 with the curvature half diameter R = 3.33D in the optimum range is especially favorable. The circular tube elbow (No 4) should not be given consideration for pneumatic conveyor installations. Insofar as the evaluation according to the parameter ζ_S is concerned, the segmental turns are in the medium spot. The four-edge tube arcs with mean curvature half diameters of about three times the channel width are rated much higher. Where R = 1.5D (No 11), the parameter ζ_S is markedly higher. In arcs of this type, the turn is facilitated by an intermediate wall (No 13). A wall of this nature is advantageous even if the half diameters are larger (No 14, in contrast to No 12). Broadening of the turn cross section in comparison to the adjoining tubes causes no significant change in the loss coefficient ζ_S (Nos 17 and 18, in comparison to Nos 15 and 16).

The four-edge tube elbow is unsuitable for the conveyance of dust-laden air. The non-stationary movement of the dust deposited in the outer corner turbulences, that falls back into the main flow in a roughly periodic sequence; this was described in an earlier report[9]. The channel elbow with rounded corners, often employed in large installations, should be executed with guding vanes in sufficiently dense shingle-like layering (No 22). The construction with two insufficiently overlapping guiding vanes (No 21) is no more favorable in terms of loss coefficient ζ_S than the channel elbow with guding sheets and chamfered edges (Nos 23 and 24).

Construction and finishing considerations

In practice, it is desirable to have both low turn losses in the air flow and constructions that are not subject to undue attrition, as well as are easy to construct. The circular tube arc has the disadvantage -- as a consequence of its large local attrition loss at the outer flank [10] and the rather expensive nature of its construction. Segmental turns are both relatively easy to manufacture and resistant to attrition losses. In the case of the four-edge tube arc, the strong local attrition loss may be compensated for by using a thicker tube wall. If an intermediate wall is fitted, then the attrition loss is distributed between this wall and the back of the turn (turn Nos 13 and 14). Favorable attrition loss distribution is achieved in the four-edge tube elbow with guiding sheets (Nos 21 to 24) also.

There exists no clear-cut trend between local attrition and turn loss. Thus, for example, the four-edge tube elbow (No 19) turned out surprisingly attrition-resistant in coal-dust conduits, whereas the tube arc --

favorable from the flow-technological angle -- exhibits an acceptably long service life only if its wall thickness is very large.

In many instances, only one of the following three requirements, viz.,

small turn loss,
attrition-resistant construction,
ease of construction,

will govern the selection of a turn configuration. In the case of small tube diameters, the circular tube arc should be given favorable consideration in most instances. If the conveyed matter is relatively soft (such as sawdust), and the tube diameters are large, then the circular tube segment turn is most suitable. On the other hand, if the conveyed substance is abrasive, the four-edge tube arc is preferable in the medium tube diameter range, and the tube elbow with guiding vanes is preferable in the large tube diameter range.

The velocity difference between dust and air

The pressure drop

$$\Delta p_S = \Delta p_U - \Delta p_{U,0} = \mu \, q \, \zeta_S$$

applies to the turning of the flow of conveyed substance. Assuming that the wall friction of the dust in the exhaust flow tube is sufficiently considered in terms of extrapolation pressure drop $(\Delta p/\Delta x)_2$, the pressure drop Δp_S will be consumed essentially for the re-acceleration of the dust that had been braked in the turns. In the course of this, the dust velocity increases from the mean value $\underline{c}$ at the exit from the turn by the amount of $\Delta c = w - c$ to the mean air velocity $\underline{w}$. The impulse increase $\dot{m}_S \, \Delta c$ of the dust flow $\dot{m}_S$ is then the same as the pressure force $\Delta p_S F$, where $\underline{F}$ denotes the constant cross section of the exhaust flow tube. Accordingly, with

$$\dot{m}_S = \mu \rho w F,$$

the following expression applies:

$$\Delta p_S F = \mu \, q \zeta_S F = \mu \rho w F \, \Delta c = 2 \, \mu q F \, (\Delta c/w) \qquad \text{or} \quad \zeta_S = 2 \, \Delta c/w$$

This simple relation connects the loss coefficient ζ_S with the increase in velocity Δc in the exhaust flow tube or with the velocity decrease of the dust in the turn that corresponds practically to the conveyed substance.

The smallest value measured in the tests, ζ_S = 1.19 (turn No 2) thus indicates that the dust velocity decreased by approximately 60%, i.e., to 40% of the mean air velocity. At the highest value of ζ_S = 2.82 (No 19), the dust velocity would have decreased by $\Delta c > w$, i.e., to a negative value. Indeed, there are instances in the four-edge and circular tube elbows where the dust progresses locally backwards.

Generalization of the test results

The turn losses relate, by definition, to a process with developed flow at the turn entry with developed flow at the exhaust flow also. In conveying systems where there are only short straight tube sections, for example between two turns in which the flow does not develop fully, there is no physically unambiguous definition of the turn losses. In cases of this type, the loss coefficients in Table 1 have only a relative meaning.

An analysis of the test results, taking into consideration the attrition traces observed in the turns investigated, leads to the assumption that no basically different findings are likely for turns with other configurations such as elliptical arcs. Thus, for example, the relatively small difference between the loss coefficients ζ_S of so widely differing turns as Nos 2 and 22 indicates that any minimum value for this coefficient would not be significantly lower than the minimum value of ζ_S = 1.19 (tube arc No 2) encountered in these studies. An increase of the cross section of the inlet tube, resulting at a lower dust entry velocity, will not cause a decrease of the turn loss coefficient ζ_S either. Delaying of the dust in the inlet flow and re-accelerating it in the turn is, according to a calculation based on an earlier study [7], more loss-producing than the process in a constant cross-section tube arc.

The preliminary tests with coal dust gave practically the same results as the tests in which quartz dust was the conveyed substance. Accordingly, it is likely that there is no substance specificity in the behavior of dusts in turns. BWK 322

Bibliography

[1] G. Weidner: "Grundsaetzliche Untersuchung ueber den Pneumatischen Foerdergang, insbesondere ueber die Verhaeltnisse bei Beschleuniging und Umlenkung" (Fundamental Study of the Pneumatic Conveying Process, Especially of the Relations Prevailing in Acceleration and Turns); Forch. Ing.-Wes., Vol 21, 1955, No 5, pp 145-153.

[2] R. Jung: "Der Druckabfall im Einlaufgebiet Pneumatischer Foerderanlagen" (The Pressure Drop in the Intake Zone of Pneumatic Convetors); Forsch. Ing-Wes. , Vol 24, 1958, No 2, pp 50-58.
[3] Huette [Engineering Handbook]; Vol 1, 28th edition, Berlin, 1955.
[4] W. Barth: "Stroemungstechnische Probleme der Verfahrenstechnik" (Flow-Technological Problems of Process Technology); Chemie-Ing.-Techn., Vol 25, 1954, No 1, pp 29-34.
[5] W. Barth: "Stroemungsvorgaenge beim Transport von Festteilchen und Fluessigkeiten in Gasen" (Flow Processes in the Transport of Solid Particles and Liquids in Gases); Chemie-Ing.-Techn., Vol 30, 1958, No 3, pp 171-180.
[6] E. Muschelknautz: "Theoretische und Experimentelle Untersuchungen ueber die Druckverluste Pneumatischer Foerderleitungen unter Besonderer Beruecksichtigung des Einflusses von Gutreibung und Gutgewicht" (Theoretical and Experimental Investigations on Pressure Losses in Pneumatic Conveyor Conduits with Especial Emphasis on the Effects of Substance Friction and Substance Weight); VDI-Forschungsheft, No 476, Duesseldorf, 1959.
[7] R. Jung: "Der Druckverlauf beim Pneumatischen Staubtransport durch ein Kreisrohr Veraenderlichen Querschnitts" (The Course of Pressure in Pneumatic Dust Transport Through a Circular Tube with Variable Cross Section); BWK, Vol 18, 1966, No 8, pp 377-383.
[8] H. Richter: "Rohrhydraulik" (Tube Hydraulics), 3rd edition, Berlin-Goettingen-Heidelberg, 1958.
[9] R. Jung: "Verbrennungstechnische Massnahmen zur Korrosionsbekaempfung in Steinkohlen-Schmelzfeuerungen" (Combustion-Technological Measures for Corrosion Prevention in Hard Coal Melt Firings); Werkstoffe u. Korrosion, Vol 16, 1965, No 10, pp 853-862.
[19] H. Brauer and E. Kriegel: "Verschleiss von Rohrkruemmern beim Pneumatischen und Hydraulischen Feststofftransport" (Attrition of Tube Turns in Pneumatic and Hydraulic Solid Substance Transport); Chemie-Ing.-Techn., Vol 37, 1965, No 3, pp 265-276.

CAPTIONS AND LEGENDS

Fig. 1. Test setup. a) Tube inlet; b) dust addition; c,d) measuring section; e) precipitation cyclone; f) exhaust air tube; g) dust collector; h) tube chute; i) funnel; k) dust rotating-tube feeder; l) turn (model curvature)

Fig. 2. Measuring section. a) Inlet tube; b) exhaust tube; c) model turn; d) pressure measuring sites; A) first pressure measuring site in a; E) last pressure measuring site in b; 0) starting point of longitudinal coordinate x.

Fig. 3. Example of a measured pressure distribution before and after a circular tube arc (Model No 1 in Table 1). Curve a for unladen air flow; curve b for the same with μ = 0.80 kg dust per kg air in the flow. Air velocity in the tube w = 33.7 m/sec; air density 1.125 kg/cu m. p_A static pressure at the first measuring site (A in Fig. 2); p static pressure at the distance x from the intersection point of the tube axes.

Fig. 4. Pressure distribution before and after a channel elbow with guiding vanes (Model No 22 in Table 1) under the same conditions as in the example shown in Fig. 3.

Fig. 5. Comparison between the measured tube friction coefficient λ_L and the Prandtl law for turbulent tube friction in developed flow.

Fig. 6. Measured related turn loss in turns No 1 and 22 (cf. Figs. 3 and 4, and Table 1) as a function of loading, μ (ζ_U = turn loss)

Fig. 7. Channel elements for the transition from round tube to turn. a) Transition from circular to equally wide square cross section (turns 11 to 14 and 17 to 24); b) transition from circular to equally large square cross section (turn 15); c) transition from circular to equally large rectangular cross section.

Fig. 8. Circular tube segmental turns.

Table 1. Dimensions and loss coefficients of the turns investigated. 1) No.; 2) designation; 3) configuration and cross section; 4) dimensions; 5) loss coefficient; 6) circular tube turns; 7) arc; 8) elbow; 9) segmental turn; 10) four-edge turns; 11) arc; 12) transition as illustrated in Fig. 7a; 13) arc with intermediate wall; 14) arc with square cross section; 15) arc with rectangular cross section; 16) see Fig. 7b and 7c; 17) arc with variable cross section; 18) elbow; 19) elbow with guiding vanes; 20) two guiding yanes; 21) five guiding vanes, see Fig. 4; 22) elbow with guding conduits; 23) two guiding conduits; 24) four guding conduits.

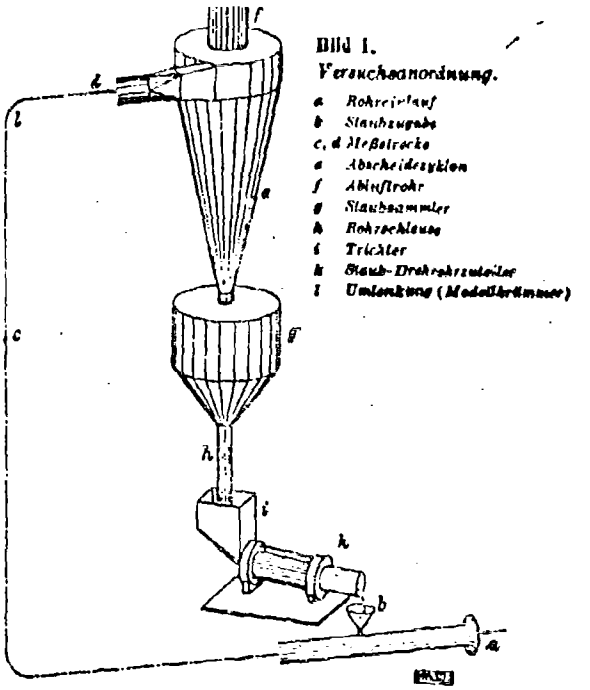

Bild 1.
Versuchsanordnung.

- *a Rohrverlauf*
- *b Staubzugabe*
- *c, d Meßstrecke*
- *e Abscheidezyklon*
- *f Abluftrohr*
- *g Staubsammler*
- *h Rohrschleuse*
- *i Trichter*
- *k Staub-Drehrohrzuteiler*
- *l Umlenkung (Modellkrümmer)*

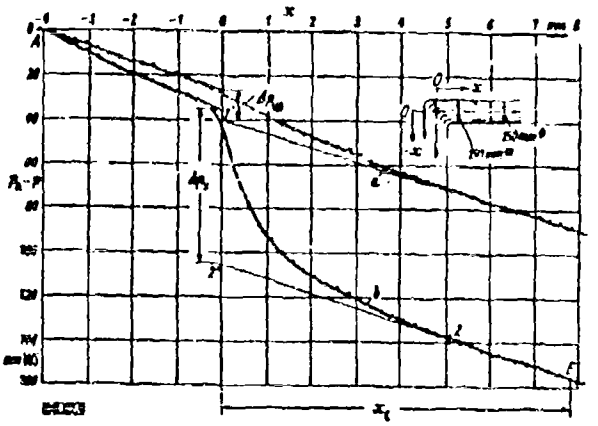

Bild 4. *Druckverteilung vor und nach einem Kanalknie mit Leitschaufeln (Modell Nr. 22 in Zahlentafel 1) unter den gleichen Bedingungen wie im Beispiel von Bild 3.*

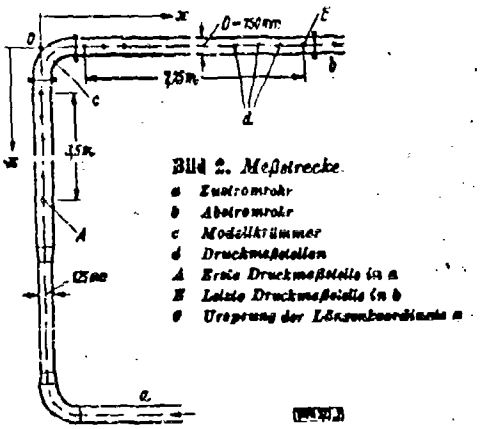

Bild 2. *Meßstrecke*

- *a Zustromrohr*
- *b Abströmrohr*
- *c Modellkrümmer*
- *d Druckmeßstellen*
- *A Erste Druckmeßstelle in a*
- *E Letzte Druckmeßstelle in b*
- *0 Ursprung der Lösungskoordinate x*

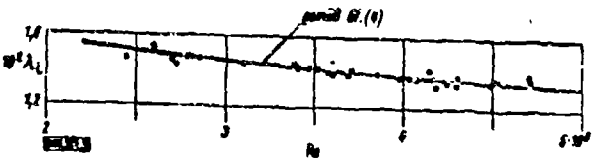

Bild 5. *Vergleich zwischen der gemessenen Rohrreibungszahl λ_L und dem Prandtlschen Gesetz der turbulenten Rohrreibung bei ausgebildeter Strömung.*

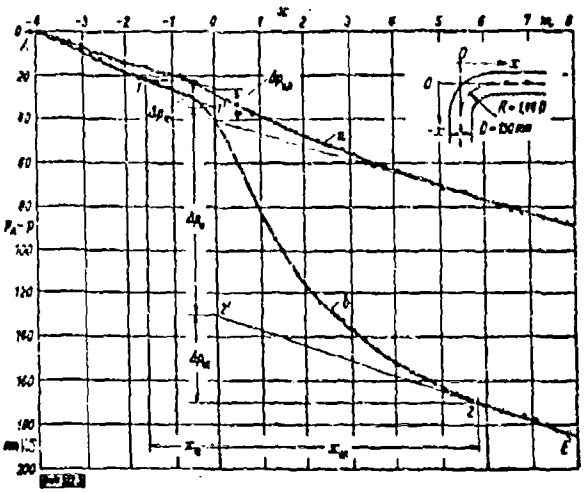

Bild 3. *Beispiel einer gemessenen Druckverteilung vor und nach einem Kreisrohrbogen (Modell Nr. 1 in Zahlentafel 1).*

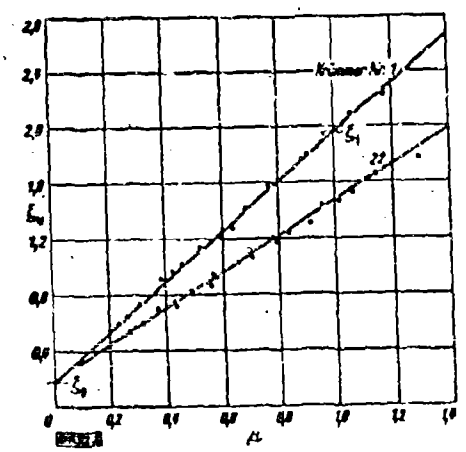

Bild 6. *An den Krümmern Nr. 1 und 22 (vgl. Bild 3, 4 und Zahlentafel 1) gemessener bezogener Umlenkverlust ζ_U in Abhängigkeit von der Beladung μ.*

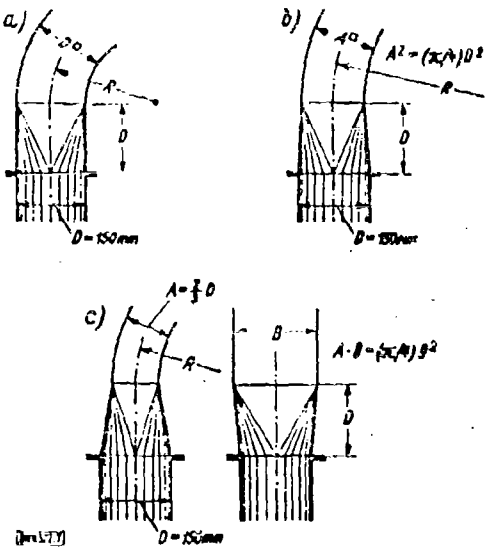

Bild 7. *Kanalelemente für den Übergang vom runden Rohr zum Krümmer.*

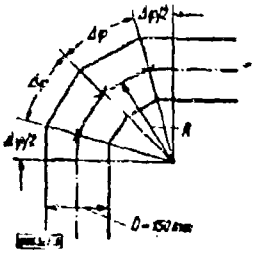

Bild 8. *Kreisrohr-Segmentkrümmer.*

Table 1. Dimensions and loss coefficients of the turns investigated. 1) No.; 2) designation; 3) configuration and cross section; 4) dimensions; 5) loss coefficient; 6) circular tube turns; 7) arc; 8) elbow; 9) segmental turn; 10) four-edge turns; 11) arc; 12) transition as illustrated in Fig. 7a; 13) arc with intermediate wall; 14) arc with square cross section; 15) arc with rectangular cross section; 16) see Fig. 7b and 7c; 17) arc with variable cross section; 18) elbow; 19) elbow with guiding vanes; 20) two guiding vanes; 21) five guiding vanes, see Fig. 4; 22) elbow with guding conduits; 23) two guiding conduits; 24) four guding conduits.

Zahlentafel 1. Abmessungen und Verlustbeiwerte der untersuchten Krümmer.

Nr.	Bezeichnung	Form u. Querschnitt	Abmessungen		Verlustbeiwert ζ_0	ζ_1	ζ_2
	Kreisrohrkrümmer						
1	Bogen	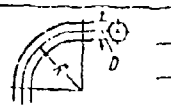	$R/D = 1{,}44$		0,17	1,08	1,70
2			3,33		0,15	1,34	1,10
3			6		0,13	1,07	1,51
4	Knie	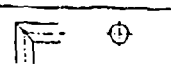	6		1,14	3,28	2,14
5	Segmentkrümmer	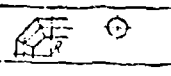	n 2	1,5	0,33	2,20	1,87
6		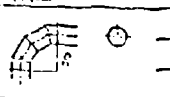	3	1,5	0,22	2,05	1,83
7			3	1,04	0,20	1,91	1,74
8			3	3	0,20	1,92	1,72
9		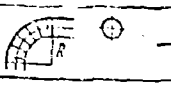	6	1,5	0,19	2,05	1,80
10			6	3	0,15	1,84	1,69
	Vierkantrohrkrümmer						
11	Bogen	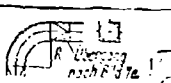	1,5		0,23	1,98	1,75
12			3		0,09	1,57	1,48
13	Bogen mit Zwischenwand		$R/D = 1{,}5$		0,13	1,55	1,42
14			3		0,12	1,40	1,37
15	Bogen mit Quadrat-	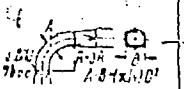	$D/A = 1$		0,15	1,61	1,36
16	mit Rechteck-Querschnitt		1,8		0,15	1,61	1,46
17	Bogen mit veränderlichem Querschnitt	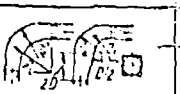	$R_1 = R_A = 2D$		0,15	1,40	1,34
18			$R_1 = D$ $R_A = 2D$		0,18	1,57	1,30
19	Knie	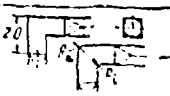			0,54	3,66	2,82
20			$R_1 = R_A = D/3$		0,56	3,17	2,91
21	Knie mit Leitschaufeln	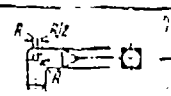	$R = D/3$ 2 Leitschaufeln		0,24	1,81	1,57
22			5 Leitschaufeln s. Bild 4		0,20	1,48	1,26
23	Knie mit Leitstegen	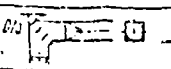	2 Leitstege		0,33	1,87	1,52
24			4 Leitstege		0,33	1,82	1,49